Title

Movable window insulation as an instantiation of the adaptive building envelope: An investigation of its cost-effectiveness in the U.S

Authors

Zeng, Zhaoyun
Chen, Jianli
Augenbroe, Godfried

Publication Date

2021-09-01

DOI

10.1016/j.enbuild.2021.111138

Peer reviewed

Movable window insulation as an instantiation of the adaptive building envelope: An investigation of its cost-effectiveness in the U.S.

Zhaoyun Zeng[1,2], Jianli Chen[3], Godfried Augenbroe[2]
1. Lawrence Berkeley National Laboratory
2. Georgia Institute of Technology
3. The University of Utah

1. Introduction

In 2017, residential buildings account for 20.4% of the total energy consumption in the U.S., the portion for commercial buildings being 18.5% [1]. Together, they make buildings the largest energy consumption sector in the U.S. One of the most important ways of reducing building energy consumption is to employ high-performance building envelope. The traditional way of making building envelop more efficient is to improve its static properties, such as U-factor, solar heat gain coefficient (SHGC), and infiltration rate. This method, called the static method, has two major limitations. Firstly, a specific envelope property tends to be advantageous in one cooling or heating season while disadvantageous in the other [2-5]. Therefore, an optimized static envelope property is merely a compromise between the different needs of different seasons. It can never be the true optimum unless in some extreme climates. Secondly, simply improving the static properties of windows by brute force is usually so expensive that the savings from the reduction of energy consumption is canceled out [6, 7].

As an alternative to the static method, the concept of adaptive building envelope (ABE) is proposed. Different from traditional building envelope whose performance hinges on its static properties, the ABE is the building envelope that "has the ability to repeatedly and reversibly change some of its functions, features or behavior over time in response to changing performance requirements and boundary conditions, and does this with the aim of improving overall building performance" [3]. The term "adaptive" is substituted by other terms like responsive, active, dynamic, intelligent, smart, interactive, kinetic, and switchable in other papers [3, 8-10], but they all convey the same concept. The advantage of the ABE over traditional building envelope is that it can change its functions to make the best of different climatic conditions and address different needs of the building. For example, an electrochromic window can switch to the colored state when there is an excess of daylight or the building requires cooling, and switch back to the bleached state when more daylight is favorable or the building requires heating [11-13]. Besides, the switch between functions for ABE is realized by means of some ingenious mechanical systems or innovative materials that have the potential of achieving lower cost than traditional high-performance building envelope.

There are two approaches to the research of ABE, top-down and bottom-up. Studies using the top-down approach focus on the development of general methods or toolchains that apply to the design or operation of various ABE technologies [10, 14-18]. These studies form the infrastructure of ABE research and can benefit a large scope of researchers. Studies using the bottom-up approach, on the other hand, discuss the characteristics of ABE based on case studies of some specific technologies and try to extract some rules or conclusions from it [19-26]. These conclusions, although less general, are grounded in real cases and have more value in application.

This study adopts the bottom-up approach and movable window insulation is selected as the ABE technology to be studied. Movable window insulation is an opaque insulation layer which can be either attached to or removed from a window according to the need, as shown in Figure 1. When attached to a

window, movable insulation can grant the window additional thermal insulation and perfect solar shading. The moving mechanism may be sliding, folding, or rolling.

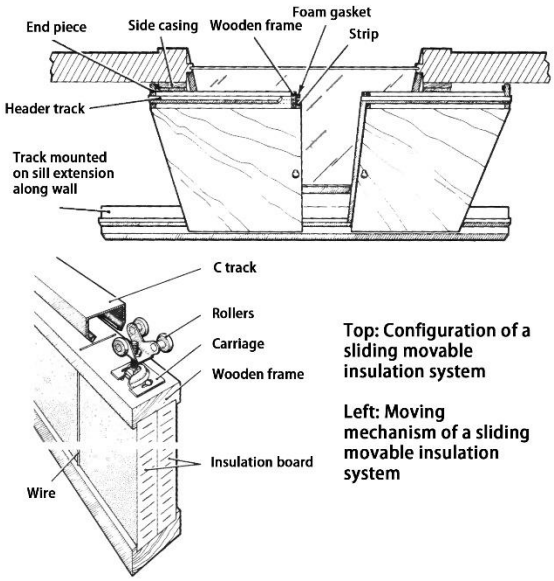

Figure 1 The configuration of an exterior sliding movable insulation system [27]

Movable window insulation is selected as the object of study due to the following three considerations. Firstly, it has a large energy-saving potential. The heating and cooling loads induced by windows, including heat transfer, solar heat gain, and infiltration due to windows, make up roughly 30% of the total heating and cooling loads of buildings [28]. By improving windows' thermal insulation and solar shading, movable insulation could potentially reduce the building thermal load significantly. Secondly, movable window insulation is able to function in multiple physical domains with relatively simple structure. Unlike most ABE systems that can only function in one physical domain, movable insulation is able to impact several physical domains including convection, radiation, lighting, and perhaps infiltration. Despite its versatility, movable insulation has relatively simple structure, which signifies low cost and easy maintenance. Thirdly, movable window insulation has not been systematically studied yet. In the 1980s, a number of application cases of movable insulation were compiled in books and guidance was given on the design and application of movable insulation [27, 29]. A preliminary experimental study on the performance of various types of window coverings was conducted [30]. Then, the research of movable insulation ceased for more than 20 years. Recently, more detailed studies on the operation, modelling, and performance of movable insulation were carried out [31-33]. One prominent feature of these studies is the application of building energy simulation (BES) programs, which is seldom seen in earlier ones. However, each of these studies only addresses a specific issue of movable insulation. A panoramic view of movable insulation is missing.

Despite its advantages, movable insulation inevitably has some disadvantages [27, 29]. The first issue is that when the insulation layer is closed, the occupants are deprived of daylight, which limits the use of movable insulation to night and the time when the room is not occupied. The second problem is that the insulation layer impedes the use of natural ventilation, which may increase electricity use of mechanical ventilation. Moreover, a narrower comfort zone is probably needed since the comfort zone predicted by the adaptive model in naturally ventilated buildings no long applies [34]. Solutions to these issues are required before the application of movable insulation.

This paper, aiming to facilitate the research and application of movable insulation, presents a comprehensive study on its cost-effectiveness. Specifically, this paper tries to answer the following questions:

- How to control movable insulation?
- How does movable insulation perform compared with static high-performance windows and electrochromic windows?
- What climate zones is movable insulation appropriate for?
- What is the energy-saving mechanism of movable insulation?
- What is the impact of infiltration on the performance of movable insulation?
- What is the payback period of movable insulation in different climate zones?

2. Methodology

This study employs BES to evaluate the energy performance of different windows.

2.1 Model

In 2019, a majority (63.9%) of U.S. households live in detached single-family buildings [35]. Therefore, the residential prototype building model developed by Pacific Northwest National Laboratory (PNNL) is adopted for this study [36]. The geometry of the prototype building model is converted from a two-story building to a one-story building with one conditioned zone and one attic, so that there is only one window on each façade. This change is done in OpenStudio [37], and will greatly reduce the difficulty of altering the model in this study. Three window-to-wall ratios (WWRs) are evaluated, which are 27.2%, 22.7%, and 18.2%. The building model after conversion has a floor area of 200 m^2, as shown in Figure 2. The construction of the building is compliant with 2012 International Energy Conservation Code (IECC) [38]. A family of three members lives in the building. The indoor environment is controlled by a packaged unit with electric cooling and gas heating. The original heating setpoint and cooling setpoint adopted by the prototype building are 22.22°C and 23.88°C, respectively. To reflect the difference in people's thermal preferences, we adopted three thermostat settings in this study. [22.22°C, 23.88°C] is the thermostat setting for occupants with a narrow comfort band and [21.22°C, 24.88°C] is the thermostat setting for occupants with a medium comfort band. For occupants with a wide comfort band, the thermostat is set as [20.22°C, 25.88°C], and if the daily outdoor air temperature is within 20°C and 26°C, the occupants will turn off the HVAC system completely for that day. The details of occupancy schedule, lighting schedule, electric equipment schedule, and gas equipment schedule can be found in [36].

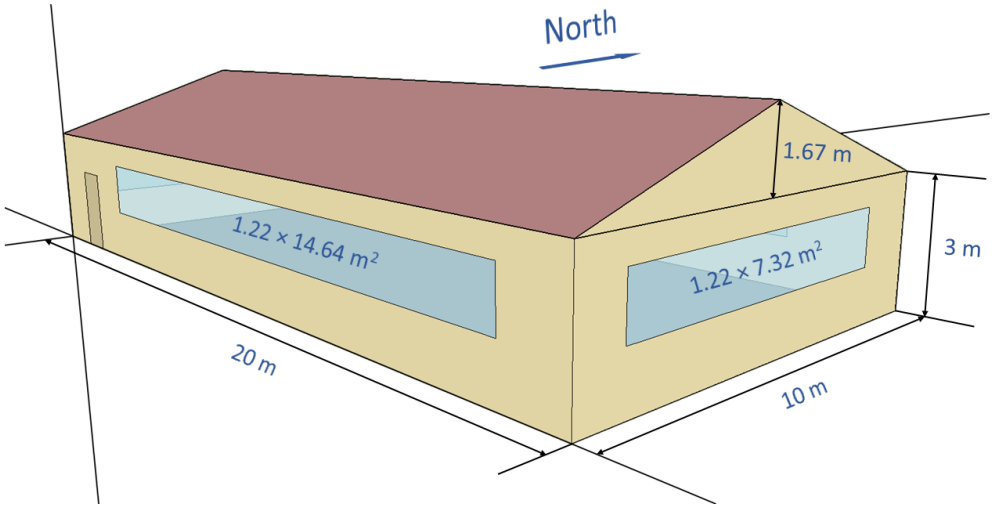

Figure 2 The dimensions of the single-family prototype building model (taking the case with a WWR of 27.2% as an example)

2.2 Scenarios

Four representative cities were chosen, as shown in Table 1. For each city, five scenarios were studied: double-glazed window (baseline), triple-glazed window, double-glazed window with automatically controlled movable insulation, double-glazed window with manually controlled movable insulation, and electrochromic window, as summarized in Table 2. Double-glazed windows are selected as the baseline and their U-factors are in compliance with IECC. The U-factor of triple-glazed windows is 0.7 W/(m^2·K), which represents a high-end triple-glazed window product on the market. For each double-glazed window and triple-glazed window, we are also interested in finding its optimal SHGC. The SHGC of a window can be altered by employing shading devices, tinted glass, or coatings [39-41]. Compared to the decrease of the U-factor, which usually relies on using more layers of glass or filling the cavity with inert gases, the change of the SHGC is much less costly [39, 40]. For double-glazed windows, there are three candidate SHGC levels: 0.25, 0.4, and 0.6. For triple-glazed windows, it is generally difficult to elevate the SHGC above 0.45 due to the extra layer of glass and the application of low-e coatings [39, 42]. Hence, there are only two candidate SHGC levels: 0.25 and 0.4. For Minneapolis where the climate is heating-dominated, the SHGC level of 0.25 is ruled out directly because of its inability to make use of solar heating. For Phoenix where the climate is cooling-dominated, the SHGC level of 0.6 is ruled out directly because it admits too much solar heat gain.

Table 1 Representative cities and their climates

City	Minneapolis, MN	San Francisco, CA	Atlanta, GA	Phoenix, AZ
Climate type	Heating-dominated	Moderate	Mixed	Cooling-dominated
Climate zone	6A	3B	3A	2B

The design of the insulation layer should take durability, fire-resistance, mold-resistance, light weight, strength, health issue, and economy into account. In this study the insulation layer is placed on the outside of the glazing because the thermal resistance of the insulation is far higher than the glazing. If the insulation is placed on the inside of the glazing, moisture will enter the space between the insulation and the glazing and condense, thus causing mold problem. The insulation layer used in this study comprises from outside to inside a layer of aluminum foil, a 4-cm-thick extruded polystyrene layer, a 1-cm-thick gypsum board, and a layer of latex paint. The aluminum foil not only protects the insulation layer from

weathering but also reduces the radiation heat transfer with its low emissivity and high solar reflectivity. The data of the material properties are from ASHRAE Handbook Fundamentals [43]. The calculated total R-value of this insulation layer is 1.40 m^2·K/W. Since the sealing of a sliding insulation layer is relatively easy (e.g. by using brush seals), its air permeability can be classified as tight according to ISO 10077-1 [44]. Based on ISO 10077-1, the U-factor of a window with an additional insulation layer is calculated by

$$U_{\mathrm{WI}} = \frac{1}{\frac{1}{U_{\mathrm{W}}} + 0.95 \times R_{\mathrm{I}} + 0.17} \quad (1)$$

where U_{WI} is the U-factor of the window with insulation [W/(m^2·K)]; U_{W} is the U-factor of the bare window [W/(m^2·K)]; R_{I} is the R-value of the insulation layer [m^2·K/W]. In Table 2, each window with movable insulation has two U-factors and two SHGCs. The former is the one when the insulation layer is open, and the latter is the one when the insulation layer is closed.

For each city, the U-factor of the electrochromic window is the same as that of the double-glazed window. The bleached-state SHGC and colored-state SHGC of the electrochromic window are 0.41 and 0.09, respectively, which are the properties of a product by SageGlass® [45]. The purpose of adding the electrochromic window to the comparison is to investigate the energy-saving potential by only controlling the SHGC of a window (compared to movable insulation whose SHGC and U-factor are controlled simultaneously).

Table 2 The properties of windows considered in this study

City	Window	U-Factor [W/(m^2·K)]	SHGC	City	Window	U-Factor [W/(m^2·K)]	SHGC
Minneapolis	Double-0.4	1.82	0.4	San Francisco	Double-0.25	1.99	0.25
	Double-0.6	1.82	0.6		Double-0.4	1.99	0.4
	Triple-0.4	0.7	0.4		Double-0.6	1.99	0.6
	MI-0.4 Auto	1.82/0.489	0.4/0		Triple-0.25	0.7	0.25
	MI-0.6 Auto	1.82/0.489	0.6/0		Triple-0.4	0.7	0.4
	MI-∗ Manual	1.82/0.489	∗		MI-0.25 Auto	1.99/0.500	0.25/0
	Electrochromic	1.82	0.41/0.09		MI-0.4 Auto	1.99/0.500	0.4/0
Atlanta	Double-0.25	1.99	0.25		MI-0.6 Auto	1.99/0.500	0.6/0
	Double-0.4	1.99	0.4		MI-∗ Manual	1.99/0.500	∗
	Double-0.6	1.99	0.6		Electrochromic	1.99	0.41/0.09
	Triple-0.25	0.7	0.25	Phoenix	Double-0.25	2.27	0.25
	Triple-0.4	0.7	0.4		Double-0.4	2.27	0.4
	MI-0.25 Auto	1.99/0.500	0.25/0		Triple-0.25	0.7	0.25
	MI-0.4 Auto	1.99/0.500	0.4/0		Triple-0.4	0.7	0.4
	MI-0.6 Auto	1.99/0.500	0.6/0		MI-0.25 Auto	2.27/0.516	0.25/0
	MI-∗ Manual	1.99/0.500	∗		MI-0.4 Auto	2.27/0.516	0.4/0
	Electrochromic	1.99	0.41/0.09		MI-∗ Manual	2.27/0.517	∗
					Electrochromic	2.27	0.41/0.09

∗ The SHGC coefficient of the double-glazed window with manually controlled movable insulation is the same as optimal SHGC of the double-glazed window with automatically controlled movable insulation.

2.3 Control

Windows on different façades are controlled independently. The diagram of the automatic control system is shown in Figure 3. The outdoor and indoor thermometers measure the outdoor and indoor temperatures, respectively. The pyranometer measures the incident solar radiation (both direct and diffuse) on each window. The black bulb temperature sensor measures the mean radiant temperature of the environment

surrounding each window. When the sun is shining, the black bulb temperature sensor should be shaded from the sun or just simply disabled. The infrared detector detects the presence of occupants (whether they are in the building and whether they are in bed). In this control logic, the access to daylight is given priority over building load reduction. Thus, the movable insulation will remain open as long as the building is occupied and the incident solar radiation on the window exceeds 20 W/m^2. The user input information, including the cooling and heating setpoints, window U-factor, window average transmittance, window average absorptance, and window outside face emissivity, is used to calculate the energy balance of the window. If the window average transmittance and window average absorptance are not available, the user can simply input the SHGC and the system will estimate these values using the method explained in [46]. The control time step is set as 15 minutes.

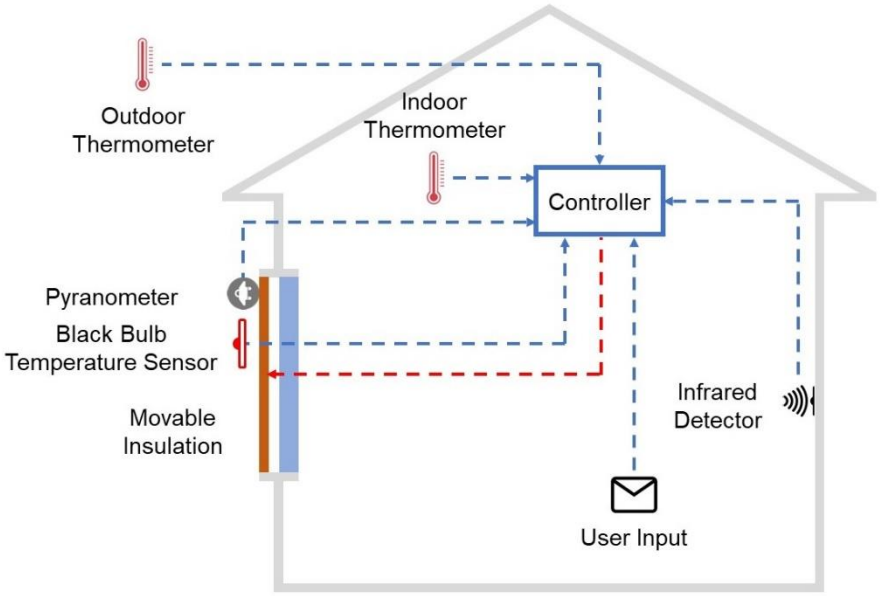

Figure 3 Diagram of the control system

The flowchart of the control algorithm is shown in Figure 4. This control algorithm is based on the energy balance calculation of the window and returns the optimal control command of the current time step. The energy balance calculation of the window follows the method used in EnergyPlus [46-48]. In this method, the glazing system is regarded as an equivalent single layer, as shown in Figure 5. The portion of incident solar radiation absorbed by the glazing system is split equally and added to surface 1 and surface 2. The heat balance equations for surface 1 and surface 2 are

$$h_{\mathrm{rad}}(T_{\mathrm{rad}} - T_1) + h_{\mathrm{o}}(T_{\mathrm{o}} - T_1) + k(T_2 - T_1) + \frac{1}{2}\alpha S = 0 \quad (2)$$

$$h_{\mathrm{i}}(T_{\mathrm{i}} - T_2) + k(T_1 - T_2) + \frac{1}{2}\alpha S = 0 \quad (3)$$

where h_{rad} is the equivalent radiation heat transfer coefficient and is calculated by $h_{\mathrm{rad}} = \sigma\varepsilon_1\left(T_{\mathrm{rad}}^2 + T_1^2\right)(T_{\mathrm{rad}} + T_1)$ [W/(m^2·K)]; σ is the Stefan–Boltzmann constant, 5.67×10^{-8} W/(m^2·K^4); ε_1 is the emissivity of surface 1; T_{rad} is the mean radiant temperature of the exterior environment [K]; T_{o}, T_1, T_2, and T_{i} are the temperatures of the outdoor air, surface 1, surface 2, and indoor environment [K], respectively; k is the equivalent thermal conductance [W/(m^2·K)], and is calculated according to [46]; α is the solar absorptance of the glazing system; S is the incident solar radiation [W/m^2]; h_{o} is the outside surface convection heat transfer coefficient [W/(m^2·K)]; h_{i} is the inside surface heat transfer coefficient that takes both convection and radiation into account [W/(m^2·K)]. From Equations (2) and (3) we can

solve for the temperatures of surface 1 and surface 2 and then the conduction heat flux through the window is calculated by

$$Q_{\mathrm{c0}} = k(T_1 - T_2) \quad (4)$$

The solar radiation transmitted through the window is calculated by

$$Q_{\mathrm{r0}} = \tau S \quad (5)$$

The transmittance of the glazing system depends on the incident angle and temperature. Here we use a single average value. The total heat transfer rate through the window when the movable insulation is open is

$$Q_0 = Q_{\mathrm{c0}} + Q_{r0} \quad (6)$$

When the movable insulation is closed, the transmittance of window is reduced to 0. All the absorbed solar radiation should be added to surface 1. The heat balance equations in this case are

$$h_{\mathrm{rad}}(T_{\mathrm{rad}} - T_1) + h_{\mathrm{o}}(T_{\mathrm{o}} - T_1) + U_{\mathrm{WI}}(T_2 - T_1) + \alpha_1 S = 0 \quad (7)$$

$$h_{\mathrm{i}}(T_{\mathrm{i}} - T_2) + U_{\mathrm{WI}}(T_1 - T_2) = 0 \quad (8)$$

Where U_{WI} is the U-factor of a window with an additional insulation layer calculated by Equation 1 [W/(m^2·K)]; α_1 is the absorptance of the exterior surface of the insulation layer. The conduction heat flux through the window in this case, Q_1, can be calculated by

$$Q_1 = U_{\mathrm{WI}}(T_1 - T_2) \quad (9)$$

When $T_{\mathrm{in}} > T_{\mathrm{cl}} - 0.5$°C, where T_{cl} is the cooling setpoint [°C], the control system will compare Q_0 and Q_1 and choose the smaller one as the movable insulation state to reduce heat gain through the window. When $T_{\mathrm{in}} < T_{\mathrm{ht}} + 0.5$°C, where T_{ht} is the heating setpoint [°C], the control system will choose the greater one of Q_0 and Q_1 as the movable insulation state to increase heat gain through the window. The reason for using $T_{\mathrm{ht}} + 0.5$°C and $T_{\mathrm{cl}} - 0.5$°C instead of T_{ht} and T_{cl} as thresholds is that with the heating ventilating and air conditioning (HVAC) system working properly, the indoor temperature will fluctuate slightly around T_{ht} when heating is on and T_{cl} when cooling is on. The adoption of $T_{\mathrm{ht}} + 0.5$°C and $T_{\mathrm{cl}} - 0.5$°C as thresholds will ensure that load reduction is always effective as long as the HVAC system is on.

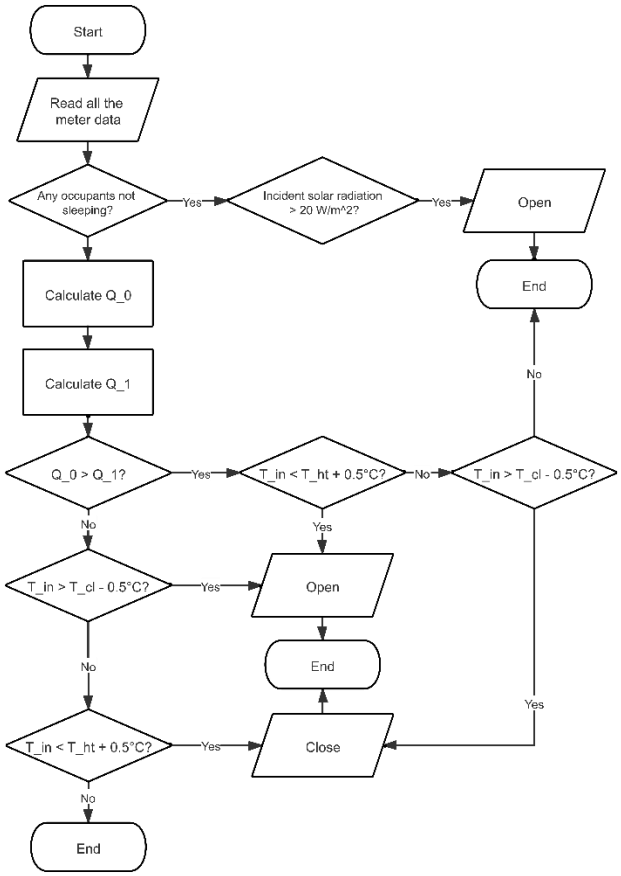

Figure 4 Flowchart of the control algorithm

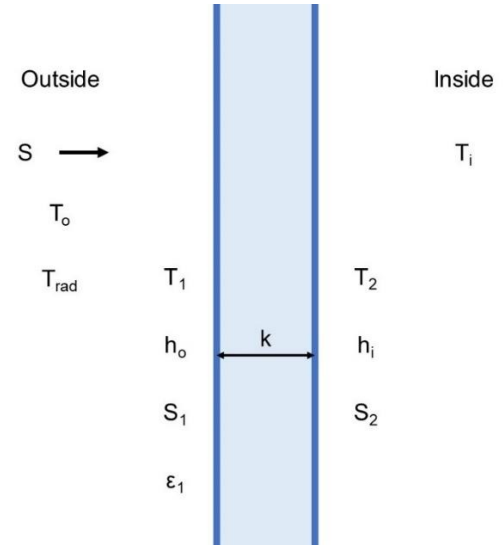

Figure 5 Diagram of the heat balance calculation when the movable insulation is open

In the manual control scenario, three assumptions are made. Firstly, the occupants have access to weather forecast of the next 4 hours and the forecast is sufficiently accurate considering such a short forecast horizon. Secondly, the occupants will control the movable insulation based on some simple rules. Thirdly,

the occupants will perform the control action at several fixed time points. As shown in Figure 6, each day is divided into 5 control steps and the schedule is different for the heating season and the cooling season. The time frame of cooling season also varies for different cities. At the beginning of each control step, the occupants will have a look at the weather forecast report and perform the control action based on the outdoor temperature and cloud cover a few hours in the future (denoted by left arrows in Figure 6). The movable insulation will keep the same state throughout a control step. The night step begins right before the occupants go to bed. In the heating season, if the outdoor temperature at 3:00 is between T_{ht} and 25°C, the insulation layers on all façades are opened. In the cooling season, the temperature range for opening movable insulation is from 18°C to T_{cl}. The two daylight steps begin right after the occupants get up and right after the occupants get home, respectively. In these two steps, the insulation layers on all façades are opened for daylight. The unoccupied step begins right before the occupants go out. In the heating season, the insulation layers on the south façade are opened if it is sunny at 13:00. In the cooling season, the insulation layers on the north façade are opened if the outdoor temperature at 13:00 is between 18°C and T_{cl}. The evening step begins after sunset. In the heating season, if the outdoor temperature at 21:00 is between T_{ht} and 25°C, the insulation layers on all façades are opened. In the cooling season, the temperature range for opening movable insulation is from 18°C to T_{cl}.

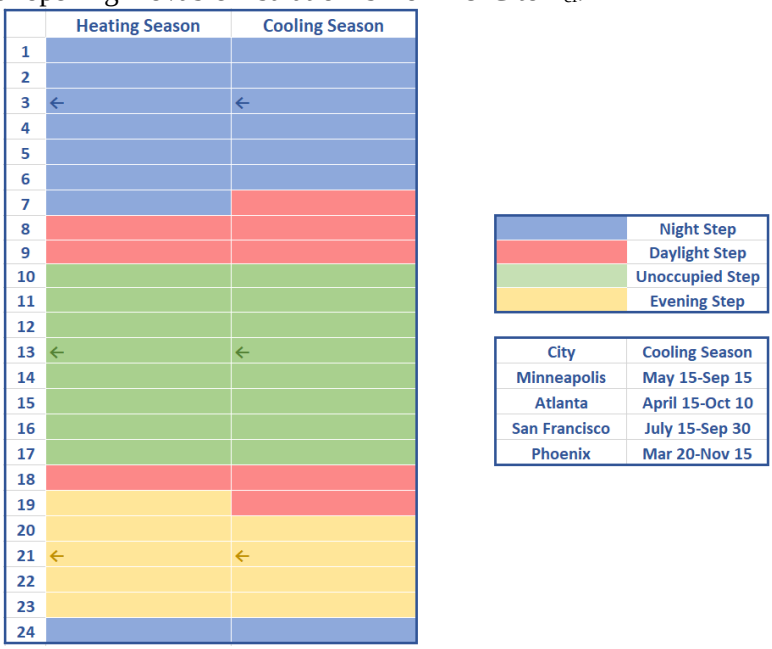

Figure 6 The control steps of manual control

The control of the electrochromic window is based on a simple rule. When the indoor temperature is lower than T_{ht} + 0.5°C, the window is switched to the bleached state. When the indoor temperature is higher than T_{cl} – 0.5°C, the window is switched to the colored state.

2.4 Simulation

The BES is conducted by EnergyPlus 8.6, which is a whole building energy modelling program developed by the National Renewable Energy Laboratory (NREL) [47]. It has been widely validated and verified [49]. The control of movable insulation and electrochromic windows is realized by the Energy Management System (EMS) module of EnergyPlus [50]. The time step of simulation is 15 minutes. At the beginning of each time step, EMS reads the sensor values of the outdoor dry-bulb temperature, sky temperature, indoor temperature, incident solar radiation rate per area on each window surface, outside radiation heat transfer coefficients (including to air, to sky, and to ground) of each window, and the occupancy schedule. Then, the EMS programs containing the control algorithms are called and the

optimal control commands are returned. Finally, the control commands are executed by an EMS actuator called Construction State. Two Construction objects are created to represent the two states (open and closed) of movable insulation (the same for electrochromic windows), and the control algorithm will select the appropriate state for each time step.

3. Results

3.1 Shading effect of nearby buildings

In BES conventions, the shading of nearby buildings is seldom modelled unless in urban-scale studies. This simplification can greatly shorten the simulation time. In this section, we test if the shading of nearby buildings has a prominent impact on the energy need of buildings. Figure 7 is the satellite image of a typical suburb in the U.S where most single-family buildings are located. The distance between a single-family building and its neighbors on the left and right is around 5 m. The neighbor in front of the building is 30 m away due to the existence of lawns and a road. Hence, we assume three buildings with the same geometry as that of the prototype building are located on the east, west, and south of it. The distance between them is 5 m, 5 m and 30 m, respectively. Since Minneapolis has the smallest solar altitude angle, which means the shading effect of nearby buildings is the strongest, we select Minneapolis as the city for this test. The WWR and comfort band for this test are 27.2% and narrow, respectively. The annual cooling/heating energy need with or without the shading of nearby buildings is shown in Table 3. For most windows, the difference between the annual cooling/heating energy need with or without the shading of nearby buildings is around 1% or 2%. Therefore, we may conclude that for buildings located in suburbs where the height and density of buildings are small, the shading effect of nearby buildings can be neglected.

Figure 7 Satellite image of a typical suburb in the U.S.

Table 3 The annual cooling/heating energy need with or without the shading of nearby buildings

Window	Cooling Electricity without Shading (kWh/m^2)	Cooling Electricity with Shading (kWh/m^2)	Heating Gas without Shading (kWh/m^2)	Heating Gas with Shading (kWh/m^2)
Double	6.98	6.80	110.84	111.52
Triple	7.60	7.39	79.74	80.36
MI Auto	4.20	4.05	76.14	76.92

MI Manual	5.05	4.87	84.51	85.09
Electrochromic	3.32	3.24	111.16	111.79

3.2 The optimal SHGC

In this section, we try to identify the optimal SHGC of each type of window in different scenarios. In order to compare the performance of windows with different SHGC, we convert both electricity and natural gas to source energy and use it as the metric. The average source-site ratios of electricity and natural gas in the U.S. are 2.8 and 1.05, respectively [51]. Figure 8 shows the HVAC source energy use intensity (EUI) of different windows in different scenarios. The comfort band has little impact on the selection of the optimal SHGC, while for different WWRs the optimal SHGC may be different. For the readers' convenience, the optimal SHGC of each type of window in different scenarios is summarized in Table 4. In Minneapolis when the WWR is 22.7% or 27.2%, the optimal SHGC for static windows is 0.4, which is in compliance with IECC, while that for windows with movable insulation is 0.6. Similar phenomena can be observed for Atlanta and San Francisco. This is because for static windows, higher SHGC is advantageous to the reduction of heating energy but adverse to the reduction of cooling energy. A balance should be stricken between the decrease of heating energy and the increase of cooling energy. Movable insulation, on the other hand, can reduce the cooling energy significantly by blocking the sunlight during the daytime on weekdays when the building is not occupied. Therefore, windows with movable insulation can have a higher SHGC than static windows to better utilize solar energy in the heating season. The IECC standard may be appropriate for static windows, but it does not apply to windows with movable insulation. Hereinafter, in the comparison between different window types only the optimal SHGC is considered.

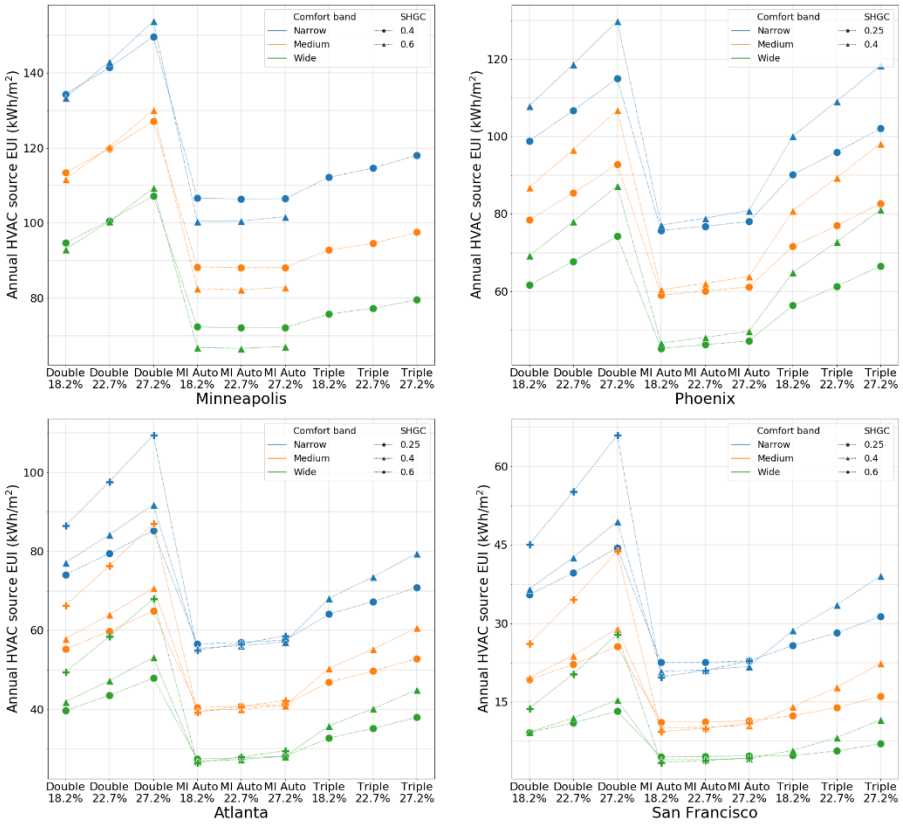

Figure 8 The HVAC source energy use intensity (EUI) of different windows in different scenarios

Table 4 – The optimal SHGC of each type of window in different scenarios

City	Window	Optimal SHGC		
		18.20%	**22.70%**	**27.20%**
Minneapolis	Double	0.6	0.4	0.4
	Triple	0.4	0.4	0.4
	MI	0.6	0.6	0.6
Phoenix	Double	0.25	0.25	0.25
	Triple	0.25	0.25	0.25
	MI	0.25	0.25	0.25
Atlanta	Double	0.25	0.25	0.25
	Triple	0.25	0.25	0.25
	MI	0.6	0.4	0.4
San Francisco	Double	0.25	0.25	0.25
	Triple	0.25	0.25	0.25
	MI	0.6	0.6	0.4

3.3 The comparison of energy performance

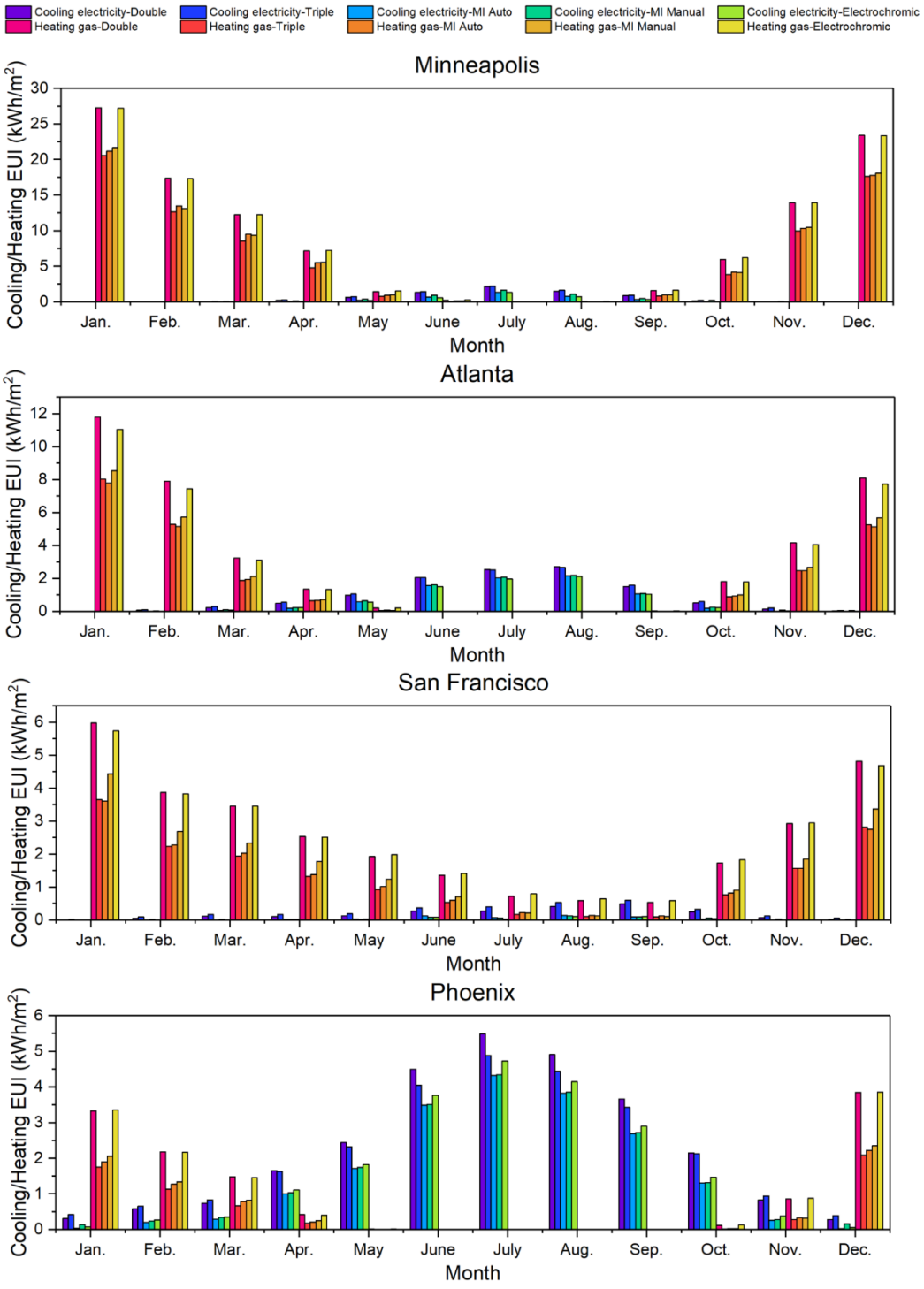

Figure 9 The monthly cooling/heating energy comparison

Figure 9 shows the monthly heating/cooling EUI for different windows when the WWR is 27.2% and the comfort band is narrow. The EUI for other scenarios follows similar patterns. In all four cities, movable insulation with automatic control has the best energy performance in terms of reducing both heating energy and cooling energy. The energy performance of movable insulation with manual control is similar to but slightly worse than that of movable insulation with automatic control. Triple-glazed windows are

effective in reducing the heating energy but perform awfully in reducing the cooling energy. In mild weathers, they are even outperformed by double-glazed windows in terms of reducing the cooling energy, because they hinder the loss of internal heat to the outside at night. Electrochromic windows, on the contrary, are effective in reducing the cooling energy but perform poorly in reducing the heating energy. Their cooling energy is the lowest in all the cities except Phoenix. From the energy performance of triple-glazed windows and electrochromic windows, we may conclude that cooling energy reduction is largely the consequence of a low SHGC, while heating energy reduction mainly relies on a low U-factor.

3.4 Elucidation of the energy-saving mechanism of movable insulation

In this section, we investigate the energy-saving mechanism of movable insulation. The scenario where the WWR is 27.2% and the comfort band is narrow is taken as an example. The same mechanism applies to all scenarios.

3.4.1 Heating gas rate

Figure 10 shows the heating gas rate profiles of different windows on two extreme winter days in Minneapolis. Figure 11 shows the movable insulation state of each window for the same time period. The presence of a color bar indicates that the insulation layer in that orientation is closed. From Figure 10 we can see that the heating gas rate profiles are roughly parallel for most of the time. The profiles reach the bottom in the afternoon, rise gradually, and reach the peak in the early morning at 6:00. There is another peak around 8:30 when the occupants leave the building and the internal heat gain drops. The profile of movable insulation with manual control has some huge spikes in the daylight steps, because the insulation layers on all windows are opened for daylight.

From Figure 11 we can see that the insulation layers on the south and east façades are opened first in the morning, followed by those on the west and north façades to let in daylight. Then, the insulation layers on the west and north façades are closed because the diffuse solar radiation transmitted through these windows is not strong enough to compensate for the convective heat loss. In the afternoon, the insulation layers on the east façade are closed and those on the west façade are opened. At dusk the insulation layers on the south façade are closed first, followed by those on the west façade.

3.4.2 Peak heating gas rate

From Table 5 we can see that the triple-glazed window and movable insulation with automatic control can reduce the peak heating gas rate by 20.8% and 25.4% respectively compared to the double-glazed window. A reduction in the peak heating gas rate leads to a smaller equipment size and hence reduces initial investment.

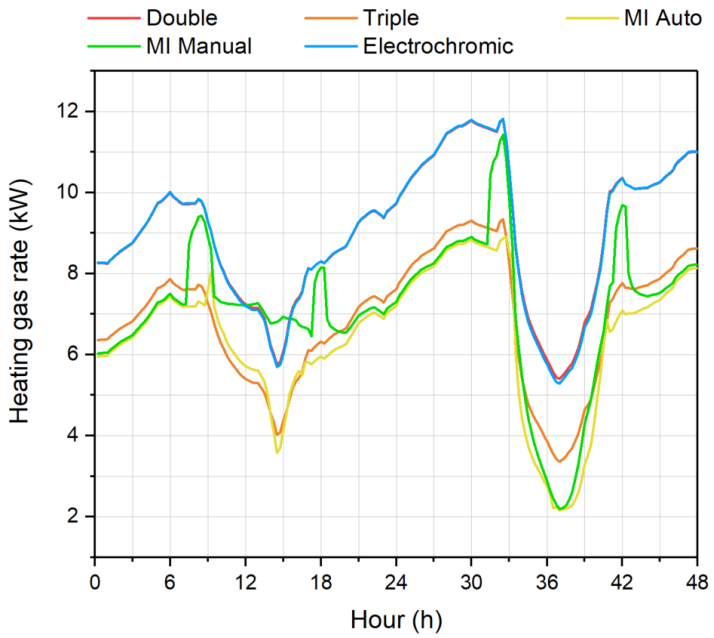

Figure 10 The heating energy profile on two typical winter days for Minneapolis

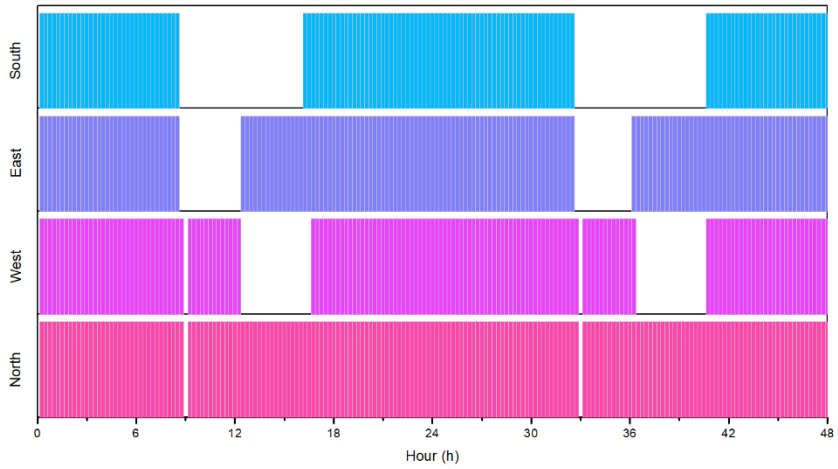

Figure 11 The movable insulation state of each window on two typical winter days for Minneapolis (the presence of the color bar indicating that movable insulation is closed.)

Table 5 The peak heating gas rate of different windows

	Double	Triple	MI Auto	MI Manual	Electrochromic
Peak heating gas rate (kW)	11.80	9.34	8.90	11.43	11.82
Percentage lower than double-glazed windows	0%	20.8%	24.5%	3.1%	–0.2%

3.4.3 Cooling electric power

Figure 12 shows the hourly cooling electric power profiles on two extreme summer days in Phoenix. Figure 13 shows the movable insulation state of each window for the same time period. From Figure 12 we can see that the profile of the double-glazed window is the highest, followed by those of the triple-

glazed window and the electrochromic window. The profiles of movable insulation with automatic control and movable insulation with manual control are the lowest for most of the time and almost coincide. However, when the occupants return home and insulation layers are opened for daylight, the profiles of movable insulation rise above that of the electrochromic window.

In Figure 13, all insulation layers are opened at 6:30 a.m. for daylight. After the occupants leave the building, all insulation layers are closed to reduce the solar and convective heat gain until the residents return home. One interesting thing to mention in Figure 13 is that the movable insulation on the southern window is closed before that on the north window at sunset. This is because the sun actually rises and falls in the north in the summer in the Northern Hemisphere.

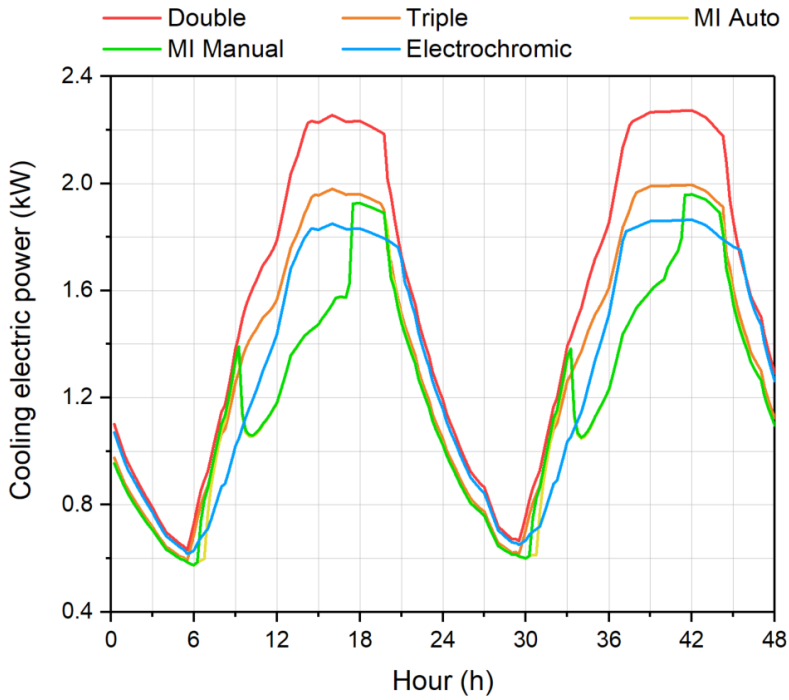

Figure 12 The cooling energy profile on two typical summer days for Phoenix

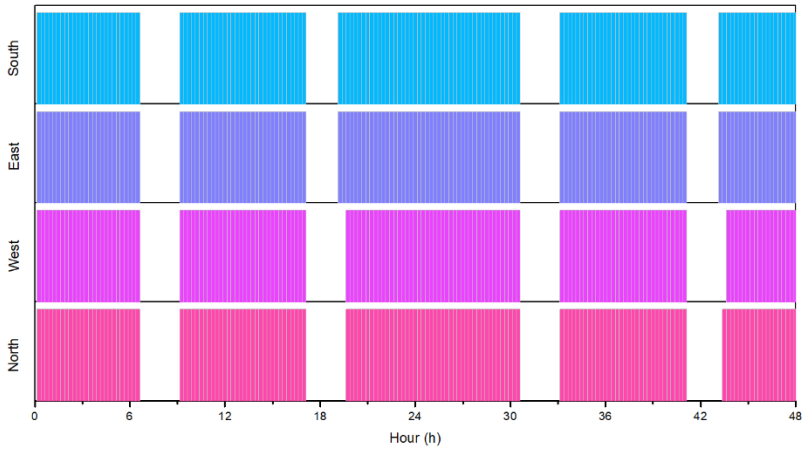

Figure 13 The movable insulation state of each window on two typical summer days for Phoenix (The presence of the color bar indicates that movable insulation is closed)

3.5 The impact of air infiltration on the performance of movable insulation

In this section, the impact of air permeability on the performance of movable insulation in different weather conditions is studied with the finite difference method. The finite difference model is shown in Figure 14. The meaning of each node is shown in Table 6. There is air exchange between nodes 1, 4 and nodes 4, 7 due to infiltration. The air exchange rate between nodes 4, 7 is held constant at 5×10^{-4} $m^3/(s\cdot m)$ to represent a well-sealed window. Seven different air exchange rates between nodes 1, 4 are modelled, which are 5×10^{-4}, 1.5×10^{-3}, 5×10^{-3}, 0.01, 0.02, 0.05, and 0.08 $m^3/(s\cdot m)$, respectively, to represent different air infiltration levels of the movable insulation. Eleven weather conditions are studied, including –20°C, –10°C, 0°C, 10°C, 15°C for the heating scenario and 30°C with/without solar radiation, 35°C with/without solar radiation, 40°C with/without solar radiation for the cooling scenario. The incident solar radiation on vertical surfaces is 500 W/m^2, which is a typical summer value at low latitudes. A relative humidity of 50% and clear sky are used to calculate the sky temperature. The convective and radiative heat transfer coefficients are consistent with those in EnergyPlus. The calculated heat transfer rates of different scenarios, including convection and infrared radiation, are shown in Figure 15. Negative heat transfer rate implicates the window loses heat to the environment, and vice versa. A window without movable insulation is also modelled. Its heat gain rates for the cooling scenario with solar radiation are not shown, because they are too large to be compared in this figure.

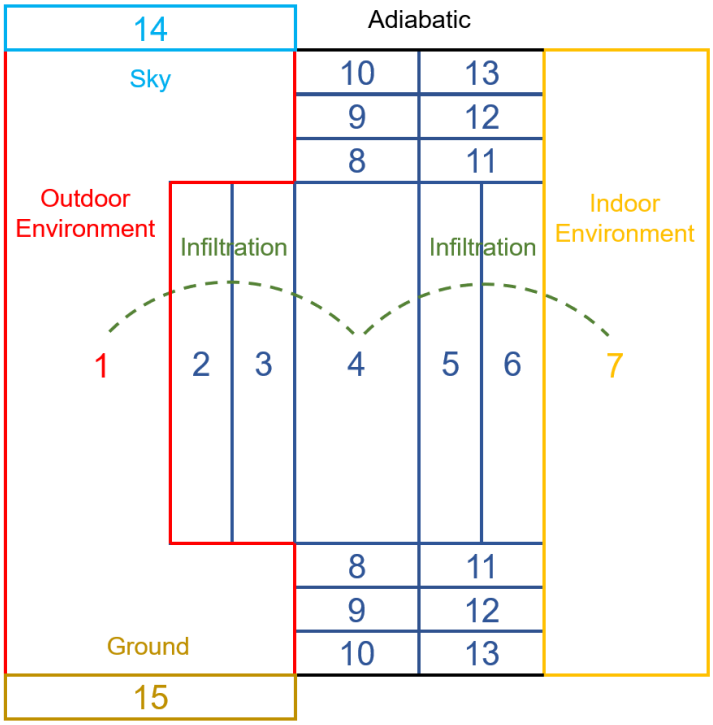

Figure 14 The diagram of the finite difference model

Table 6 The meaning of each node

Node	1	2, 3	4	5, 6
Meaning	Ambient temperature	Insulation layer	Space between the glazing and the insulation layer	Glazing
Node	7	8–13	14	15
Meaning	Indoor temperature	Wall	Sky temperature	Ground

In Figure 15, the profiles with different colors represent heat transfer rates in different weather conditions. We can see that in all scenarios except 30°C and 35°C with solar radiation, the heat transfer rate increases with the infiltration rate. When the infiltration rate rises from 5×10^{-4} to 0.01 $m^3/(s\cdot m)$, the heat transfer rate increases dramatically. Above 0.01 $m^3/(s\cdot m)$, the heat transfer rate becomes relatively stable. This is because in all scenarios except 30°C and 35°C with solar radiation, when the infiltration rate is below 0.01 $m^3/(s\cdot m)$ larger infiltration rate will make the temperature of node 4 closer to the outdoor temperature, hence increasing the convective heat transfer rate. Above 0.01 $m^3/(s\cdot m)$, the temperature of node 4 is already very close to the outdoor temperature. Further increasing the infiltration rate will only increase the heat transfer rate marginally.

In the scenarios where the temperature is 30°C or 35°C and there is solar radiation, higher infiltration rate will reduce the heat transfer rate. This is because the difference between the outdoor air temperature and the indoor cooling setpoint (23.88°C) is not so significant. With small infiltration rate, the space between the insulation and the glazing will act like a heat trap, and the temperature of the air inside it will rise above the outdoor temperature. Therefore, higher infiltration rate will reduce the convective heat transfer rate.

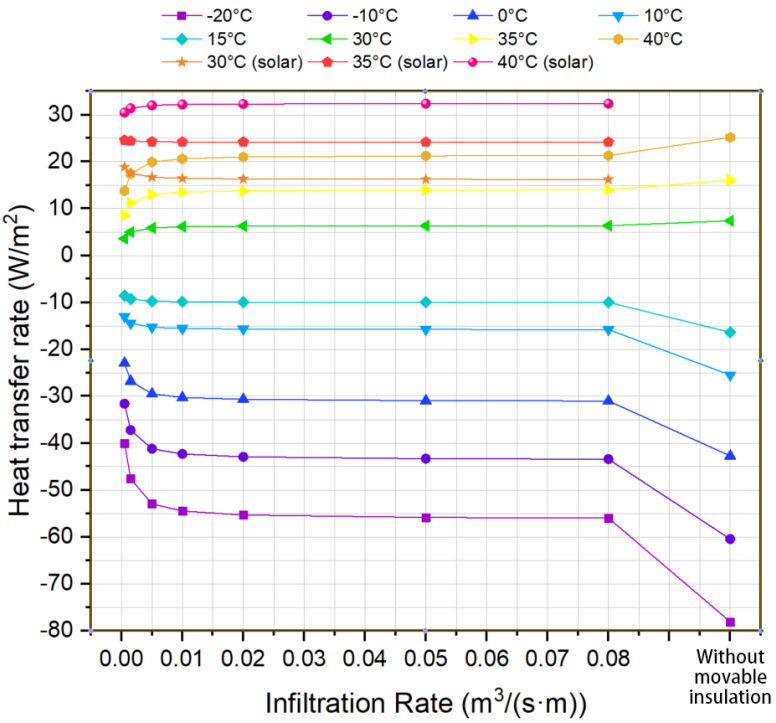

Figure 15 The heat transfer rate of the window (convection and infrared radiation) with different infiltration rates and in different weather conditions

In all scenarios even when the infiltration rate is at the highest value, 0.08 $m^3/(s\cdot m)$, the heat transfer rate is still markedly smaller than that of the window without movable insulation. This is because the insulation layer can block the radiative heat transfer between the window and the outdoor environment. In cooling scenarios, the insulation layer can block the sunlight as well as the thermal radiation from the ground. In heating scenarios, the insulation layer can block the radiative heat loss of the window to the sky, whose temperature can get below –40°C in clear winter nights, while the temperature of the inner surface of the insulation layer is at worst –10.9°C.

In conclusion, it is of great importance to improve the airtightness of movable insulation for any heating scenario. For cooling scenarios, if the location has a mild cooling season like San Francisco, it is recommended to open the movable insulation and just use proper shading devices.

3.5 NPV analysis

A net present value (NPV) analysis was conducted for different windows in different cities. The NPV of a window is calculated by

$$\mathrm{NPV} = -M_{inv} + \sum_{i=1}^{n} \frac{M_e}{(1+d)^i} \quad (10)$$

where M_{inv} is the increment in the investment of the window compared to the baseline (double-glazed window) [U.S. $]; M_e is the annual energy savings of the building compared to the baseline [U.S. $]; n is the number of years in which the NPV is evaluated; d is the discount rate. A negative NPV indicates the investment in the window has not paid back yet. As the number of evaluated years increases, the NPV increases as well, for more energy savings are taken into account. The number of years that it takes for the NPV to just become positive is the payback period.

Since the prices of building components and energy are highly volatile, we adopt a range of values for each of them in the calculation of NPV. The total energy cost includes the electricity cost of the cooling system and the fans and the natural gas cost of the heating system. The heat content of natural gas (38.64 MJ/m^3 or 1037 Btu/ft^3) is the average of the U.S. national average values over the past 5 years from the Energy Information Administration (EIA) website [52]. The range of electricity price is [$0.1199/kWh, $0.1336/kWh], where $0.1199/kWh and $0.1336/kWh are the minimum and maximum of the U.S. national average electricity price over the past 5 years, respectively [53]. Similarly, the range of natural gas price is [$0.0273/kWh, $0.0612/kWh] [54].

In RSMeans Building Construction Cost Data 2016 (North America's leading construction cost database) [55], the cost of a double-glazed window with a size of 1.83 m×1.22 m is estimated to be $725, which is used as the reference value in the determination of the ranges of costs of different windows. A ±10% variation range is applied to the cost of double-glazed windows with $725 as the mean. Based on the cost data from several papers [6, 7], it is reasonable to assume that the cost of triple-glazed windows is in the range of [120%, 140%] of the reference value. In 2005 and 2006, the price of electrochromic windows was around 10 times that of static solar controlled windows [56, 57]. Over the past decade, the price of electrochromic windows has been dropping significantly. In 2016, most of the smart windows (not necessarily electrochromic windows) cost between $538/m^2 ($50/ft^2) and $1076/m^2 ($100/ft^2) [58]. In the news posted in 2018, electrochromic windows were said to cost 2 to 4 times as much as standard double-paned windows [59, 60]. Therefore, we adopt a range of [150%, 250%] × $725 for the cost of electrochromic windows. The building in question requires 24 windows in total.

The estimated cost of the insulation layer is $47.79/m^2 as detailed in Table 7. These values are also from RSMeans Building Construction Cost Data 2016 [55]. Similar to double-glazed windows, a ±10% variation range is applied to the cost of the insulation layer with $47.79/m^2 as the mean. The total cost of the control system is $657 as detailed in Table 8. The prices of its components are typical values offered by multiple manufacturers on an e-commerce website frequently used by small businesses [61]. Considering the volatility of the prices of commodities sold online, we assume a ±20% variation range for the total cost of the control system with $657 as the mean. The total cost of movable insulation with automatic control is the sum of the costs of the insulation layers and the control system, while the total cost of movable insulation with manual control only contains that of the insulation layers. Besides, the

discount rate used by U.S. Department of Energy for projects related to energy conservation, renewable energy resources, and water conservation is 3% [62]. Considering the discount rate depends on economic conditions and government policies, we assume a variation range of [2%, 4%] for it. 5 levels are adopted for each cost value and 3 levels are adopted for the discount rate. This is equal to the assumption of uniform distributions for all the random variables. No actual distributions are applied as they are unknown [63]. The levels of the random variables are summarized in Table 9. In total, 540,000 NPV cases are investigated.

Table 7 Cost of materials used in the insulation layer

Material	XPS 5.08 cm	Gypsum board 1 cm	Latex	Aluminium foil
Cost ($/m^2)	22.17	10.66	4.42	10.54

Table 8 Cost of the components of the control system

Item	Thermometer	Infrared detector	Pyranometer	Actuator	Controller	Black bulb temperature sensor	Wire
Unit price (U.S. $)	5	3.5	100	40	30	20	50
Number	2	2	4	4	1	4	1

Table 9 The levels of the random variables

	Unit	Levels				
Natural gas	$/kWh	0.0273	0.0357	0.0442	0.0527	0.0612
Electricity	$/kWh	0.1199	0.1233	0.1268	0.1302	0.1336
Double-glazed window	$/Unit	652.5	688.75	725	761.25	797.5
Triple-glazed window	$/Unit	870	906.25	942.5	978.75	1015
Insulation layer	$/m^2	43.011	45.401	47.79	50.180	52.569
Control system	$/Set	525.6	591.3	657	722.7	788.4
Electrochromic window	$/Unit	1087.5	1268.75	1450	1631.25	1812.5
Discount rate	%	2		3	4	

The payback periods of different windows in different scenarios are shown in Figure 16. Payback periods longer than 100 years are all marked as 100 years, as they mean the same, i.e., not a good option, to the home owner. We use box-whisker plots to show the distribution of calculated payback periods. In all four cities, windows with automatically or manually controlled movable insulation have the shortest payback periods. Manual control is slightly better than automatic control because of its low initial investment. Only in some scenarios do triple-glazed windows have payback periods shorter than 100 years. For electrochromic windows, the payback period is never shorter than 100 years, indicating that at their current prices, electrochromic windows are not a profitable investment from pure energy point of view. However, their ability to modulate the daylight without blocking the view to the outside may justify their application in some cases.

Both the WWR and the comfort band have certain influence on the payback period but the influence of the latter is greater. Wider comfort bands lead to longer payback periods. The reason is that the cost of windows does not vary with comfort bands, while the annual HVAC energy savings decrease with wider

comfort bands. The impact of the WWR on the payback period is more significant for movable insulation with automatic control than that for movable insulation with manual control. This is because the cost of the former comprises two parts, i.e., the fixed cost (the control system) and the variable cost (the insulation layer), while the cost of the latter only comprises the variable cost. The fixed cost is constant regardless of the window area, while the variable cost increases linearly with the window area. Hence, for movable insulation with automatic control, a smaller window area signifies a higher cost per unit area.

In Minneapolis, the median payback period of triple-glazed windows is 33 years and, in some cases, where the cost of triple-glazed windows is low and the cost of energy is high, the payback period is shorter than 20 years. Considering a lifespan of 20 years for most window products [64], triple-glazed windows may be a profitable option in Minneapolis. The variation ranges of the payback period are much smaller for movable insulation with automatic control and movable insulation with manual control. The median payback period is 11 years for both of them, showing their great application potential in extremely cold climates. In Phoenix, triple-glazed windows are not recommended due to payback periods longer than 100 years. The median payback periods for movable insulation with automatic control and movable insulation with manual control are 16 and 12 years, respectively, which proves that movable insulation is also a good choice in extremely hot climates. In Atlanta, installing triple-glazed windows are not a prudent investment. The median payback periods for movable insulation with automatic control and movable insulation with manual control are 23 and 19 years, respectively, which means that in most of the cases installing movable insulation is profitable and manual control is preferred economically over automatic control. In San Francisco, triple-glazed windows are not a good choice. For movable insulation, the payback period is around 25 years when the comfort band is narrow and much longer for other comfort bands. This is primarily due to the mild climate of the city. Since the annual energy consumption is already small for double-glazed windows, investing in advanced windows is unnecessary.

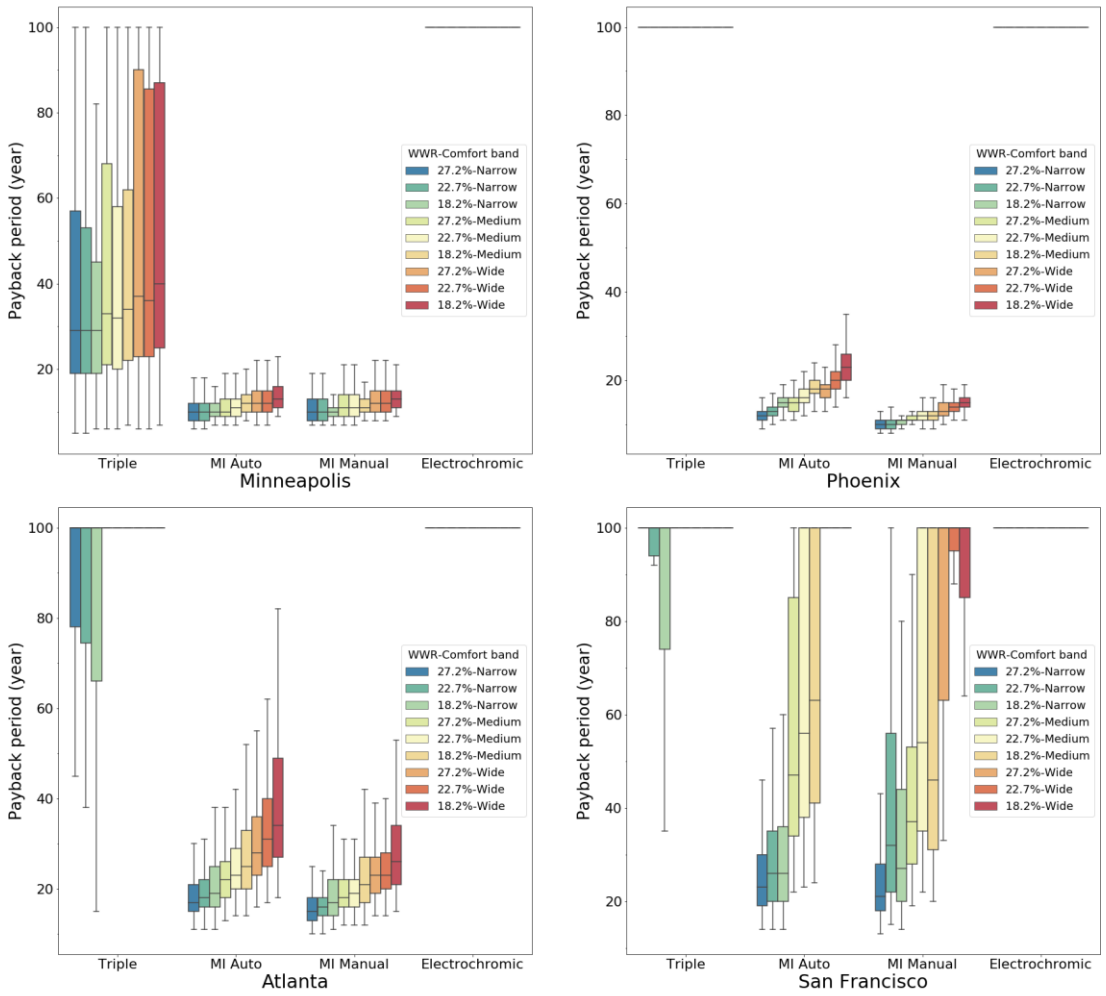

Figure 16 The box-whisker plot of payback periods of different windows in different scenarios

4. Discussion

This paper presents a systematic study on movable insulation, including its control, the parameters impacting its performance, and its cost-effectiveness compared to other static and smart windows. Nevertheless, this paper has some limitations.

Firstly, only four cities in the US were studied due to the limitation of time and resource. However, these four cities are representative of cooling-dominated, mixed, moderate, and heating-dominated climates. The conclusion drawn from these cities can be easily generalized to other cities in similar climates.

Secondly, the manual control of movable insulation is idealized. We assume the occupants change the state of insulation layers five times a day at fixed time points and the decision is made based on weather forecast. In reality, the occupants may change the state of insulation layers arbitrarily even with guidance available. Therefore, the occupants' behavior is hard to predict and may have a negative impact on the performance of movable insulation. Although movable insulation with manual control is the most cost-effective option in most cities, automatic control probably should be selected instead considering the occupants' reluctance to control movable insulation manually.

Lastly, this paper studies the energy performance of movable window insulation in single-family buildings, which represent the housing choice of 63.9% U.S. households (U.S. Census Bureau, 2020). Compared to its application in single-family buildings, the application of movable insulation in commercial buildings faces more challenges. Commercial buildings like office buildings usually have a higher requirement for daylight during the day, which limits the use of insulation panels. During the night these buildings are usually unoccupied and unconditioned, leaving not much room for load reduction. Moreover, installing insulation panels on the exterior surface of commercial buildings may be prohibited due to aesthetic concerns, fire safety requirement or falling risk.

5. Conclusions

Several issues that are critical to the application of movable insulation are discussed in this study. An automatic control system is proposed for movable insulation. A manual control rule requiring only limited control actions is also proposed, whose energy performance is comparable to that of automatic control.

By means of BES, we find that the SHGC requirement of IECC does not apply to windows with movable insulation. In some cases, a SHGC higher than the required value may result in lower energy consumption. Triple-glazed windows are effective in reducing the heating energy but perform awfully in reducing the cooling energy. Electrochromic windows, on the contrary, are effective in reducing the cooling energy but perform poorly in reducing the heating energy. We may conclude that cooling energy reduction is largely the consequence of a low SHGC, while heating energy reduction mainly relies on a low U-factor. Movable insulation excels in reducing both heating and cooling energy need. In Minneapolis, triple-glazed windows and movable insulation with automatic control can both reduce the peak heating gas rate remarkably.

The airtightness of movable insulation is of great importance to any heating scenario. For cooling scenarios, if the location has a mild cooling season like San Francisco, it is recommended to open the insulation layers and just use proper shading devices.

The payback periods of windows are influenced by a number of uncertain factors. From an economic point of view, electrochromic windows are not a good option in any city. Triple-glazed windows are a viable option only in some cases in Minneapolis. The payback period of movable insulation is smaller than 20 years in most cases in Minneapolis, Phoenix, and Atlanta, showing its great application potential in these cities. Due to its mild climate, advanced windows are unnecessary in San Francisco.

Reference

1. U.S. Energy Information Administration. *U.S. energy flow, 2017*. 2018; Available from: https://www.eia.gov/totalenergy/data/monthly/pdf/flow/total_energy.pdf.
2. Apte, J., D. Arasteh, and Y.J. Huang. *Future advanced windows for zero-energy homes*. in *ASHRAE Transactions*. 2003.
3. Loonen, R.C.G.M., et al., *Climate adaptive building shells: State-of-the-art and future challenges.* Renewable & Sustainable Energy Reviews, 2013. **25**: p. 483-493.
4. Grynning, S., et al., *Windows in the buildings of tomorrow: Energy losers or energy gainers?* Energy and Buildings, 2013. **61**: p. 185-192.
5. Gasparella, A., et al., *Analysis and modelling of window and glazing systems energy performance for a well insulated residential building.* Energy and Buildings, 2011. **43**(4): p. 1030-1037.

6. Menzies, G.F. and J.R. Wherrett, *Multiglazed windows: potential for savings in energy, emissions and cost.* Building Services Engineering Research and Technology, 2005. **26**(3): p. 249-258.
7. Pikas, E., M. Thalfeldt, and J. Kurnitski, *Cost optimal and nearly zero energy building solutions for office buildings.* Energy and Buildings, 2014. **74**: p. 30-42.
8. Favoino, F., M. Overend, and Q. Jin, *The optimal thermo-optical properties and energy saving potential of adaptive glazing technologies.* Applied Energy, 2015. **156**: p. 1-15.
9. Heiselberg, P., *ECBCS Annex 44 Integrating Environmentally Responsive Elements in Buildings Project Summary Report*. 2012, International Energy Agency: St Albans, UK.
10. Loonen, R.C.G.M., *Approaches for computational performance optimization of innovative adaptive façade concepts* in *Department of the Built Environment*. 2018, Technische Universiteit Eindhoven: Eindhoven, the Netherlands.
11. Baetens, R., B.P. Jelle, and A. Gustavsen, *Properties, requirements and possibilities of smart windows for dynamic daylight and solar energy control in buildings: A state-of-the-art review.* Solar Energy Materials and Solar Cells, 2010. **94**(2): p. 87-105.
12. Lee, E.S. and A. Tavil, *Energy and visual comfort performance of electrochromic windows with overhangs.* Building and Environment, 2007. **42**(6): p. 2439-2449.
13. Georg, A., et al., *Switchable windows with tungsten oxide.* Vacuum, 2008. **82**(7): p. 730-735.
14. Favoino, F., Q. Jin, and M. Overend, *Design and control optimisation of adaptive insulation systems for office buildings. Part 1: Adaptive technologies and simulation framework.* Energy, 2017. **127**: p. 301-309.
15. Corbin, C.D., G.P. Henze, and P. May-Ostendorp, *A model predictive control optimization environment for real-time commercial building application.* Journal of Building Performance Simulation, 2013. **6**(3): p. 159-174.
16. Evins, R., *Multi-level optimization of building design, energy system sizing and operation.* Energy, 2015. **90**: p. 1775-1789.
17. Loonen, R.C.G.M., et al., *Simulation-based support for product development of innovative building envelope components.* Automation in Construction, 2014. **45**: p. 86-95.
18. Zeng, R., et al., *New concepts and approach for developing energy efficient buildings: Ideal specific heat for building internal thermal mass.* Energy and Buildings, 2011. **43**(5): p. 1081-1090.
19. Saeli, M., et al., *Energy modelling studies of thermochromic glazing.* Energy and Buildings, 2010. **42**(10): p. 1666-1673.
20. Henze, G.P., C. Felsmann, and G. Knabe, *Evaluation of optimal control for active and passive building thermal storage.* International Journal of Thermal Sciences, 2004. **43**(2): p. 173-183.
21. Hoffmann, S., E.S. Lee, and C. Clavero, *Examination of the technical potential of near-infrared switching thermochromic windows for commercial building applications.* Solar Energy Materials and Solar Cells, 2014. **123**: p. 65-80.
22. Kasinalis, C., et al., *Framework for assessing the performance potential of seasonally adaptable facades using multi-objective optimization.* Energy and Buildings, 2014. **79**: p. 106-113.
23. Wright, J.A., et al., *Multi-objective optimization of cellular fenestration by an evolutionary algorithm.* Journal of Building Performance Simulation, 2014. **7**(1): p. 33-51.
24. El Mankibi, M., et al., *Numerical modeling of thermal behaviors of active multi-layer living wall.* Energy and Buildings, 2015. **106**: p. 96-110.
25. Joe, J., et al., *Optimal design of a multi-story double skin facade.* Energy and Buildings, 2014. **76**: p. 143-150.
26. Gratia, E. and A. De Herde, *Optimal operation of a south double-skin facade.* Energy and Buildings, 2004. **36**(1): p. 41-60.
27. Langdon, W.K., *Movable Insulation: A Guide to Reducing Heating and Cooling Losses Through the Windows in Your Home*. 1980, Emmaus, US: Rodale Press.
28. Arasteh, D., et al. *Zero Energy Windows*. 2006. United States.

29. Shurcliff, W.A., *Thermal shutters and shades: over 100 schemes for reducing heat-loss through windows*. 1980, Baltimore, US: Brick House Pub. Co.
30. Nicol, K., *The thermal effectiveness of various types of window coverings.* Energy and Buildings, 1986. **9**(3): p. 231-237.
31. Liu, M., K.B. Wittchen, and P.K. Heiselberg, *Control strategies for intelligent glazed façade and their influence on energy and comfort performance of office buildings in Denmark.* Applied Energy, 2015. **145**: p. 43-51.
32. Liu, M., et al., *Development of a simplified and dynamic method for double glazing façade with night insulation and validated by full-scale façade element.* Energy and Buildings, 2013. **58**: p. 163-171.
33. Hashemi, A. and S. Gage, *Technical issues that affect the use of retrofit panel thermal shutters in commercial buildings.* Building Services Engineering Research and Technology, 2012. **35**(1): p. 6-22.
34. de Dear, R.J. and G.S. Brager, *Developing an Adaptive Model of Thermal Comfort and Preference.* ASHRAE Transactions, 1998. **104**.
35. U.S. Census Bureau. *2019 American Housing Survey Data Now Available*. 2020; Available from: https://www.census.gov/newsroom/press-releases/2020/2019-american-housing-survey.html.
36. Pacific Northwest National Laboratory. *Residential Prototype Building Models*. 2013 July 11, 2013; Available from: https://www.energycodes.gov/development/residential/iecc_models.
37. National Renewable Energy Laboratory. *OpenStudio*. 2019; Available from: https://www.openstudio.net/.
38. International Code Council, *2012 International Energy Conservation Code*. 2011, ICC.
39. Jelle, B.P., et al., *Fenestration of today and tomorrow: A state-of-the-art review and future research opportunities.* Solar Energy Materials and Solar Cells, 2012. **96**: p. 1-28.
40. Manz, H., S. Brunner, and L. Wullschleger, *Triple vacuum glazing: Heat transfer and basic mechanical design constraints.* Solar Energy, 2006. **80**(12): p. 1632-1642.
41. Berning, P.H., *Principles of design of architectural coatings.* Applied Optics, 1983. **22**(24): p. 4127-4141.
42. Arasteh, D., et al., *Performance criteria for residential zero energy windows.* 2006.
43. American Society of Heating Refrigerating and Air-Conditioning Engineers, *2013 ASHRAE Handbook: Fundamentals*. 2013, ASHRAE: Atlanta, GA.
44. International Organization for Standardization, *ISO 10077-1: Thermal performance of windows, doors and shutters — Calculation of thermal transmittance — Part 1: General*. 2006, ISO.
45. SageGlass®, *Performance & Acoustical Data*, in *Internet*.
46. Arasteh, D., C. Kohler, and B. Griffith, *Modeling windows in Energy Plus with simple performance indices*. 2009, Lawrence Berkeley National Laboratory.
47. U.S. Department of Energy, *EnergyPlus™ Version 8.6 Documentation -- Engineering Reference*. 2016.
48. Winkelmann, F.C. *Modeling Windows in EnergyPlus*. in *Building Simulation 2001*. 2001. Rio de Janeiro: IBPSA.
49. U.S. Department of Energy. *Testing and Validation | EnergyPlus*. 2015; Available from: https://energyplus.net/testing.
50. U.S. Department of Energy, *EnergyPlus™ Version 8.6 Documentation -- Application Guide for EMS*. 2016.
51. ENERGY STAR, *ENERGY STAR Portfolio Manager Technical Reference: Source Energy*. 2020.
52. U.S. Energy Information Administration. *Heat Content of Natural Gas Consumed*. 2020; Available from: https://www.eia.gov/dnav/ng/ng_cons_heat_a_EPG0_VGTH_btucf_a.htm.
53. U.S. Energy Information Administration. *Electricity Data Browser*. 2020; Available from: https://www.eia.gov/electricity/data/browser/#/topic/7?agg=2,0,1&geo=g&freq=M&start=200101&end=201912&ctype=linechart&ltype=pin&rtype=s&maptype=0&rse=0&pin=.

54. U.S. Energy Information Administration. *U.S. Price of Natural Gas Delivered to Residential Consumers*. 2020; Available from: https://www.eia.gov/dnav/ng/hist/n3010us3m.htm.
55. Plotner, S.C., et al., *RSMeans Building Construction Cost Data 2016*. 2015, Rockland, MA, US: RSMeans.
56. Syrrakou, E., S. Papaefthimiou, and P. Yianoulis, *Environmental assessment of electrochromic glazing production.* Solar Energy Materials and Solar Cells, 2005. **85**(2): p. 205-240.
57. Lee, E.S., et al., *A design guide for early-market electrochromic windows*. 2006, Lawrence Berkeley National Laboratory: Berkeley, California, USA.
58. Home Ideas. *How Much Do Smart Windows Cost?* 2016; Available from: https://modernize.com/home-ideas/32437/smart-windows-cost.
59. Vance, A. *Saudi-Backed Vision Fund Invests $1.1 Billion in a Maker of 'Smart Window' Glass*. 2018; Available from: https://www.bloomberg.com/news/articles/2018-11-02/saudi-backed-vision-fund-invests-1-1-billion-in-a-maker-of-smart-window-glass.
60. Wesoff, E. *Tintable-Glass Unicorn Gets Massive $1.1 Billion Investment From SoftBank Vision Fund*. 2018; Available from: https://www.greentechmedia.com/articles/read/view-gets-massive-1-1-billion-investment-from-softbank?utm_medium=email&utm_source=Daily&utm_campaign=GTMDaily#gs.KvT0YSNi.
61. Alibaba Inc. *Find quality Manufacturers, Suppliers, Exporters, Importers, Buyers, Wholesalers, Products and Trade Leads from our award-winning International Trade Site*. 2020 [cited 2020 July 27]; Available from: www.alibaba.com.
62. Lavappa, P.D. and J.D. Kneifel, *Energy Price Indices and Discount Factors for Life-Cycle Cost Analysis - 2018* 2018, National Institute of Standards and Technology.
63. Fosas, D., et al., *Mitigation versus adaptation: Does insulating dwellings increase overheating risk?* Building and Environment, 2018. **143**: p. 740-759.
64. Sbar, N., et al., *Progress toward durable, cost effective electrochromic window glazings.* Solar Energy Materials and Solar Cells, 1999. **56**(3): p. 321-341.